Cytotechnology (2024) 76:153–166
https://doi.org/10.1007/s10616-023-00605-y

ARTICLE

Evodiamine ameliorates intervertebral disc degeneration through the Nrf2 and MAPK pathways

Tian Xie · Xi Gu · Ruijie Pan · Wenzhuo Huang · Sheng Dong

Received: 17 March 2023 / Accepted: 28 October 2023 / Published online: 27 December 2023

Abstract Degradation of extracellular matrix (ECM), reactive oxygen species (ROS) production, and inflammation are critical players in the pathogenesis of intervertebral disc degeneration (IDD). Evodiamine exerts functions in inhibiting inflammation and maintaining mitochondrial antioxidant functions. However, the biological functions of evodiamine and its related mechanisms in IDD progression remain unknown. The IDD-like conditions in vivo were stimulated via needle puncture. Hematoxylin and eosin staining, Safranin O/Fast Green staining and Alcian staining were performed to determine the degenerative status. The primary nucleus pulposus cells (NPCs) were isolated from Sprague–Dawley rats and then treated with tert-butyl peroxide (TBHP) to induce cellular senescence and oxidative stress. The cell viability was assessed by cell counting kit-8 assays. The mitochondria-derived ROS in NPCs was evaluated by MitoSOX staining. The mitochondrial membrane potential in NPCs was identified by JC-1 staining and flow cytometry. The expression of collagen II in NPCs was measured by immunofluorescence staining. The levels of mRNAs and proteins were measured by RT-qPCR and western blotting. The Nrf2 expression in rat nucleus pulposus tissues was measured by immunohistochemistry staining. Evodiamine alleviated TBHP-induced mitochondrial dysfunctions in NPCs. The enhancing effect of TBHP on the ECM degradation was reversed by evodiamine. The TBHP-stimulated inflammatory response was ameliorated by evodiamine. Evodiamine alleviated the IDD process in the puncture-induced rat model. Evodiamine promoted the activation of Nrf2 pathway and inactivated the MAPK pathway in NPCs. In conclusion, evodiamine ameliorates the progression of IDD by inhibiting mitochondrial dysfunctions, ECM degradation and inflammation via the Nrf2/HO-1 and MAPK pathways.

Keywords Intervertebral disc degeneration · Evodiamine · Inflammation · Extracellular matrix · Mitochondrion · Nrf2 · MAPK

Tian Xie and Xi Gu have contributed equally to this work.

T. Xie (✉) · X. Gu
Department of Orthopedics, Wuhan Hospital of Traditional Chinese Medicine, No. 49 Lihuangpi Road, Jiang'an District, Wuhan 430014, China
e-mail: xietiandoctor@hotmail.com

R. Pan · W. Huang · S. Dong
College of Acupuncture and Bone Injury, Hubei University of Chinese Medicine, Wuhan 430061, China

Introduction

Low back pain (LBP) represents a highly prevalent contributor of disability worldwide (Global 2017). Lumbar intervertebral disc herniation (LDH), a well-known spinal disease characterized by motor and sensory impairments, is the most frequently diagnosed condition associated with LBP (Global

2016). LDH is estimated to affect 20–50 individuals per 1000 adults annually, and the most severely affected are people aged 30–50 years (Dydyk et al. 2023; Jordan et al. 2011). Intervertebral disc degeneration (IDD) serves as the most common cause of LDH (Dydyk et al. 2023). Smoking, genetic disposition, infection, deformity, and mechanical trauma are critical pathogenic factors that induce the occurrence of IDD. Current available therapeutics for IDD include conservative and surgical treatments. However, these standard treatments for IDD can only relieve the pain of patients and fail to reverse the occurrence of IDD (Xin et al. 2022). Therefore, a better understanding of underlying mechanisms involved in IDD pathogenesis and exploration of novel effective therapeutic options for IDD are urgent.

The intervertebral disc (IVD), a fibrocartilaginous tissue that lies between two vertebrae and functions as a shock-absorber, consists of nucleus pulposus (NP), annulus fibrosus (AF) and cartilage endplates. The NP is crucial to maintain the biomechanical function of IVD by counteracting and dissipating compressive loads, which depends on the extracellular matrix (ECM) secreted by nucleus pulposus cells (NPCs) (Hayes et al. 2001). In normal IVDs, the anabolism and catabolism of the ECM are in a dynamic balance. The destruction of ECM is usually induced by excessive catabolism and inadequate anabolism, which are evidenced by a disintegrin-like and metalloproteinase thrombospondin type 1 motif 4 (ADAMTS-4), matrix metalloproteinase 3 (MMP-3), matrix metalloproteinase 13 (MMP-13), collagen II (COL II) and aggrecan (Risbud and Shapiro 2014). Dysregulation of ECM content is correlated with early-stage disc degeneration, leading to inflammation (Bermudez-Lekerika et al. 2022). Interleukin-1β (IL-1β) is the most important cytokine in the IL-1 family, and it has been confirmed that the level of IL-1β increases as IDD progression in both animals and humans (Maitre et al. 2005; Kepler et al. 2013). IL-1β generation can induce the production of multiple proinflammatory mediators, such as inducible nitric oxide synthase (iNOS), cyclooxygenase 2 (COX-2), tumor necrosis factor (TNF-α), and IL-6, leading to the imbalance of ECM metabolism and inflammatory response (Millward-Sadler et al. 2009). ECM degradation and inflammation are termed as the hallmarks of IDD (Raj 2008). Thus, it is critical to promote the secretion of ECM components as well as anti-inflammatory responses to combat IDD.

Reactive oxygen species (ROS), caused by external stimuli including pro-inflammatory cytokines, nutrition deprivation and mechanical loading, is another crucial intermediator of the occurrence and progression of IDD (Bai et al. 2020). Under physiological conditions, there exists a firm antioxidant defense in response to irritation of ROS in the human body. This protective mechanism is believed to be derived from the antioxidant system and the nuclear factor erythroid 2-related factor (Nrf2)/heme oxygenase (HO-1) pathway. Upon stress initiates, Nrf2 prevents stress-induced detriment by inducing the transcription of antioxidant genes including HO-1 and NAD(P)H quinone oxidoreductase 1 (NQO1) (Lee 2018). Mitochondria is an essential source of ROS in cells. Moderate levels of mitochondrial ROS can activate the antioxidant compensation mechanism, protecting organelles from harmful effects of ROS and ultimately achieving metabolic balance (Shin et al. 2020). However, when external conditions change, overproduction of ROS can induce mitochondrial membrane depolarization and oxidative stress, affecting the biological functions of NPCs, promoting the production of inflammatory mediators and ultimately accelerating ECM degradation (Dimozi et al. 2015). ROS accumulation in NPCs can also activate the mitogen-activated protein kinase (MAPK) pathway, which then promotes the expression of inflammatory mediators and ECM degradation (Ge et al. 2020). The extracellular signal-regulated kinases 1 and 2 (ERK 1/2), c-Jun amino-terminal-kinase (JNK) and $p38^{MAPK}$ are three enzymes of the MAPK pathway that most commonly occur in studies (Johnson and Lapadat 2002). Tert-butyl hydroperoxide (TBHP) is an exogenous ROS donor and is widely used to stimulate an oxidative microenvironment in vitro (Li et al. 2022; Guo et al. 2021). Thus, we treated NPCs with TBHP to stimulate oxidative stress in vitro.

Evodia is the fruit originating from the plant *Evodia rutaecarpa*. Anti-inflammatory, analgesic, antidiarrhea, anti-vomiting, anti-ulcer, and central nervous system protecting activities are primary properties of Evodia (Son et al. 2015). Evodiamine is actively expressed in Evodia. As reported, evodiamine attenuates the lipopolysaccharide-stimulated pulmonary inflammation and fibrosis (Ye et al. 2021), protects against inflammation and airway remodeling in

asthmatic rats (Wang et al. 2021), and alleviates neuropathic pain through suppressing inflammation and improving the antioxidant functions of mitochondria (Wu and Chen 2019). However, the biological functions of evodiamine and its related mechanisms in IDD progression remain uncertain.

In the current study, we detected the biological functions of evodiamine in TBHP-treated NPCs and rat IDD models and its related mechanisms. We hypothesized that evodiamine might prevent the progression of IDD, which supports evodiamine as a promising therapeutic drug for the treatment of IDD.

Methods

Informed consent

N/A Because the paper doesn't involve any experiments with human.

Animals

Sprague–Dawley (SD) rats (male, 4 or 8 weeks old; BetterBiotechnology, Jiangsu, China) were housed under standard conditions (a 12 h light/dark cycle, 25 ± 1 °C, 50 ± 5% humidity) with free access to food and water. The experimental protocols were granted approval from the Ethics Committee of Wuhan Myhalic Biotechnology Co., Ltd (No. 202007109) and abided by the National Institutes of Health Guide for the Care and Use of Laboratory Animals.

Isolation, culture and treatment of rat nucleus pulposus cells (NPCs)

For isolating NPCs, SD rats (4 weeks old) were injected excessive sodium pentobarbital (100 mg/kg) and euthanized. The isolation of primary NPCs was conducted as previously described (Kong et al. 2021). Briefly, the spinal column was removed in sterile conditions. Then the AF-derived gel-like NP tissue was digested with 0.01% trypsin (Boyao Biotechnology, Shanghai, China) for 30 min at 37 °C, and treated with 0.125% collagenase II (Sino Biological, Beijing, China) for 4 h. Subsequently, the digested tissue was filtered using a 100-μm cell strainer. The separated NPCs were washed twice using phosphate buffered saline (PBS; Solarbio, Beijing, China) and incubated in Dulbecco's modified Eagle medium (DMEM; Solarbio) with 10% fetal bovine serum (FBS; Absin Biotech, Shanghai, China) and 1% penicillin/streptomycin in a 37 °C-atmosphere containing 5% CO_2. The medium was replaced every 3 days, and NPCs between passage one and passage three were harvested for subsequent use.

The cells (5×10^5 cells/ml) were inoculated into the culture flask. To stimulate an oxidative stress microenvironment in vitro, the NPCs were treated with 50 μM TBHP (Best-reagent, Sichuan, China) for 24 h. To detect the effect of evodiamine on TBHP-treated NPCs, the cells were pretreated with 10 μM evodiamine (Sigma-Aldrich, St-Louis, MO, USA) or 30 μM evodiamine for 2 h before TBHP treatment.

Cell counting kit-8 (CCK-8) assays

The cells incubated in 96-well plates (5×10^3 cells/well) were treated with 0 μM, 1 μM, 10 μM, 30 μM and 50 μM of evodiamine, respectively (Sigma-Aldrich). After 24 or 48 h intervention, the cells were subjected to PBS washing. Then serum-free DMEM (100 μl) containing 10 μl CCK-8 solution (Yeasen Biotechnology, Shanghai, China) was added to each well. After the plates were incubated at 37 °C for 2 h, the absorbance at 450 nm was measured using a spectrophotometer (Molecular Devices, Shanghai, China).

Measurement of mitochondria-derived ROS

For mitochondria-derived ROS evaluation, the cells were seeded into a 24-well plate (2×10^5 cells/well) and cultured with MitoSox solution (5 μM; Invitrogen, Carlsbad, CA, USA) dissolved in Hanks' Balanced Salt solution modified with calcium and magnesium (Sigma-Aldrich) at 37 °C. After 10 min of incubation, the fluorescence was imaged using a fluorescence microscope (Olympus, Tokyo, Japan) and the fluorescence intensity was determined by ImageJ software (Bethesda, MD, USA).

Measurement of mitochondrial membrane potential (MMP)

For MMP detection, the cells were incubated overnight in a 24-well plate (5×10^5 cells/well) at 37 °C with 5% CO_2. After incubation, the cells were labelled with 5 μM/l of the membrane potential probe

JC-1 (Beyotime, Shanghai, China) for 20 min at 37 °C with 5% CO_2. The changes of MMP were analyzed by flow cytometry.

Immunofluorescence

The cells were seeded into a 12-well plate (1×10^5 cells/well). After PBS washing, the cells were fixed with 4% paraformaldehyde for 15 min at room temperature and permeabilized with 0.1% Triton X-100 (Sigma-Aldrich) for 10 min. After blocking with 1% goat serum for 1 h at room temperature, the cells were incubated overnight with a primary antibody against Collagen II (ab34712, 1:200; Abcam) at 4 °C and then incubated with a HRP-conjugated secondary antibody for 2 h at room temperature. Subsequently, the cells were labelled with 4′,6-diamidino-2-phenylindle (DAPI; Sigma-Aldrich) for 5 min. Images were obtained using a fluorescence microscope and analyzed using ImageJ software.

Western blotting

Total protein was extracted from the NPCs and NP tissues using RIPA lysis buffer (Sigma-Aldrich) with a protease and phosphate inhibitor cocktail (ApexBio Technology, Shanghai, China). An Enhanced BCA Protein assay kit (Yeasen) was prepared for measurement of the protein concentration. Protein samples (30 μg) were separated by sodium dodecyl sulphate-polyacrylamide gel electrophoresis and then transferred onto polyvinylidene difluoride membranes. After blocked using 5% skimmed milk., the membranes were incubated overnight with primary antibodies against Aggrecan (ab3773, 1:800; Abcam), MMP-3 (ab52915, 1:1000; Abcam), ADAMTS-4 (ab185722, 1:1000; Abcam), MMP-13 (ab39012, 1:3000, Abcam), β-actin (ab8226, 1 μg/ml; Abcam), iNOS (ab178945, 1:1000; Abcam), COX2 (ab179800, 1:2000; Abcam), Nrf2 (ab92946, 1:1000; Abcam), NQO1 (ab80588, 1:!0000; Abcam), HO-1 (ab52947, 1:2000; Abcam), p38 (ab170099, 1:2000; Abcam), p-p38 (ab4822, 1:1000; Abcam), GAPDH (ab181602, 1:10000; Abcam), JNK (ab11074, 1:1000; Abcam), p-JNK (ab131499, 1:1000; Abcam), ERK1/2 (ab184699, 1:10000; Abcam), p-ERK1/2 (ab278538, 0.1 μg/ml; Abcam), and Lamin B1 (ab16048, 0.1 μg/ml; Abcam) at 4 °C. Then the membranes were incubated with corresponding secondary antibodies for 2 h at room temperature and subsequently subjected to TBST (Sigma-Aldrich) washing (three times and 10 min each time). The blots were developed using enhanced chemiluminescence (Yeasen) and imaged using the chemiluminescence detection system (Bio-Rad, Hercules, CA, USA).

RT-qPCR

The total RNA was isolated from NPCs using the TRIzol reagent (Invitrogen) according to the manufacturer's instructions. A Nanodrop spectrophotometer (DeNovix, Wilmington, DE, USA) was used to examine the concentration and quality of the isolated RNA. The reverse transcription into cDNA was accomplished using the PrimerScript RT Reagent kit (Beijing Think-Far Technology, Beijing, China). RT-qPCR was performed using an Applied Biosystems QuantStudio 5 Real-Time PCR System (Applied Biosystems, Foster City, CA, USA). GAPDH served as the internal reference. The relative expression level was calculated using the $2^{-\Delta\Delta Ct}$ method (Livak and Schmittgen 2001). The primer sequences used in this study were listed in Table 1.

Animal model of IDD

SD rats (male, eight weeks of age) were anesthetized with 2–3% isoflurane, followed by sterilization of tail skin using iodinated polyvinylpyrrolidone. For the needle-stab injury model, the Co8-9 tail IVD was punctured using a 20-guage needle that was inserted approximately 5 mm from the dorsal towards ventral side, rotated 360° and maintained in a fixed position for 30 s before being removed. Penicillin was injected

Table 1 Sequences of primers used for reverse transcription-quantitative PCR

Genes	Sequences (5′ → 3′)
TNF-α forward	GCCTCTTCTCATTCCTGCTT
TNF-α reverse	TGGGAACTTCTCATCCCTTTG
IL-6 forward	ACTTCACAAGTCGGAGGCTT
IL-6 reverse	AGTGCATCATCGCTGTTCAT
IL-1β forward	CACCTTCTTTTCCTTCATCTTTG
IL-1β reverse	GTCGTTGCTTGTCTCTCCTTG TA
GAPDH forward	AACTCCCATTCTTCCACCT
GAPDH reverse	TTGTCATACCAGGAAATGAGC

into the operational animals to prevent postoperative infection.

The rats were divided into four groups: (a) sham, the rats were not subjected to needle stab or drug treatment; (b) IDD, the rats underwent needle stab and received a weekly intraperitoneal injection of PBS containing DMSO; (c) IDD + Evodiamine, the rats were intraperitoneally injected with PBS containing evodiamine (40 mg/kg) weekly after IDD induction. The doss of evodiamine was chosen according to a previous study (Wang et al. 2021). Each group had six rats.

Histopathological analysis

After 4 weeks, the rats were anesthetized by intraperitoneal injection of over-dose 4% pentobarbital and sacrificed, followed by collection of tails. Then, the collected tails were fixed in 4% paraformaldehyde for 24 h, decalcified for 48 h using a rapid decalcification solution containing formic acid, formaldehyde and hydrochloric acid, and cut in the middle of the vertebrae to obtain intact IVDs. Thereafter, the sections were stained with safranin O/Fast Green (Solarbio), hematoxylin and eosin (H&E) (Sigma-Aldrich) and Alcian blue (Beyotime). The cellularity and morphology of the IVD were examined by two experienced histological researchers in a blinded manner using a microscope (Mao et al. 2011).

Immunohistochemistry examination

The rat discs were fixed in 4% paraformaldehyde, decalcified, dehydrated, cleared with dimethylbenzene and embedded in paraffin. The embedded samples were then sectioned to 5 μm-thick slices and incubated with 3% hydrogen peroxide to block endogenous peroxidase activity for 10 min and 5% bovine serum albumin to block nonspecific binding sites for 30 min at 37 °C. Subsequently, the sections were incubated with a primary antibody against Nrf2 (ab313825, 1:100; Abcam) at 4 °C overnight, and then incubated with a biotinylated secondary antibody for 10 min at room temperature. Thereafter, the sections were developed with 3,3′-diaminobenzidine (DAB) solution (Sigma-Aldrich) and counterstained with hematoxylin. Histological images were acquired with a light microscope. The intensity was quantified using the ImageJ software.

Statistical analysis

All experiments were performed at least three independent repeats. Statistical analysis was analyzed using GraphPad Prism 8 (GraphPad Software, San Diego, CA, USA). Data were described as the mean ± standard deviation. The significance between two groups was analyzed using Student's *t* test. The comparisons among multiple groups were analyzed by one-way analysis of variance followed by Tukey's *post hoc* analysis. $p < 0.05$ was considered statistically significant.

Results

Evodiamine alleviates TBHP-induced mitochondrial dysfunctions in NPCs

The chemical structure of evodiamine was presented in Fig. 1A. To assess whether evodiamine has cytotoxic effects on NPCs, the NPCs were treated with ascending concentrations of evodiamine (0, 1, 10, 30 and 50 μM) for 24 and 48 h, and the viability was assessed by CCK-8 assays. The results revealed that evodiamine significantly impaired cell viability at the dose of 50 μM, whereas no obvious difference in the viability of NPCs treated with 0 μM-30 μM was observed (Fig. 1B). Therefore, we chose concentrations of 10 μM and 30 μM for use in the subsequent experiments. Mitochondrial dysfunction is involved in the pathogenesis of IDD. When confronting with oxidative stress, mitochondrion is the primary target attacked by ROS (Youle and Bliek 2012). Therefore, we first evaluated the mitochondrial ROS by MitoSOX staining and quantified the fluorescence intensity. The results demonstrated that TBHP treatment remarkably increased the mitochondrial ROS in NPCs. However, such promotion was abolished by evodiamine dose-dependently (Fig. 1C). Based on this finding, we detected if evodiamine could maintain the MMP, which would be reduced by inner mitochondrial membrane permeabilization. The JC-1 staining and flow cytometry analysis revealed that the TBHP-induced reduction of MMP was prevented by evodiamine in a dose-dependent manner (Fig. 1D). These results demonstrate that evodiamine inhibits the TBHP-induced increase in mitochondrial ROS and alleviates mitochondrial dysfunctions in NPCs.

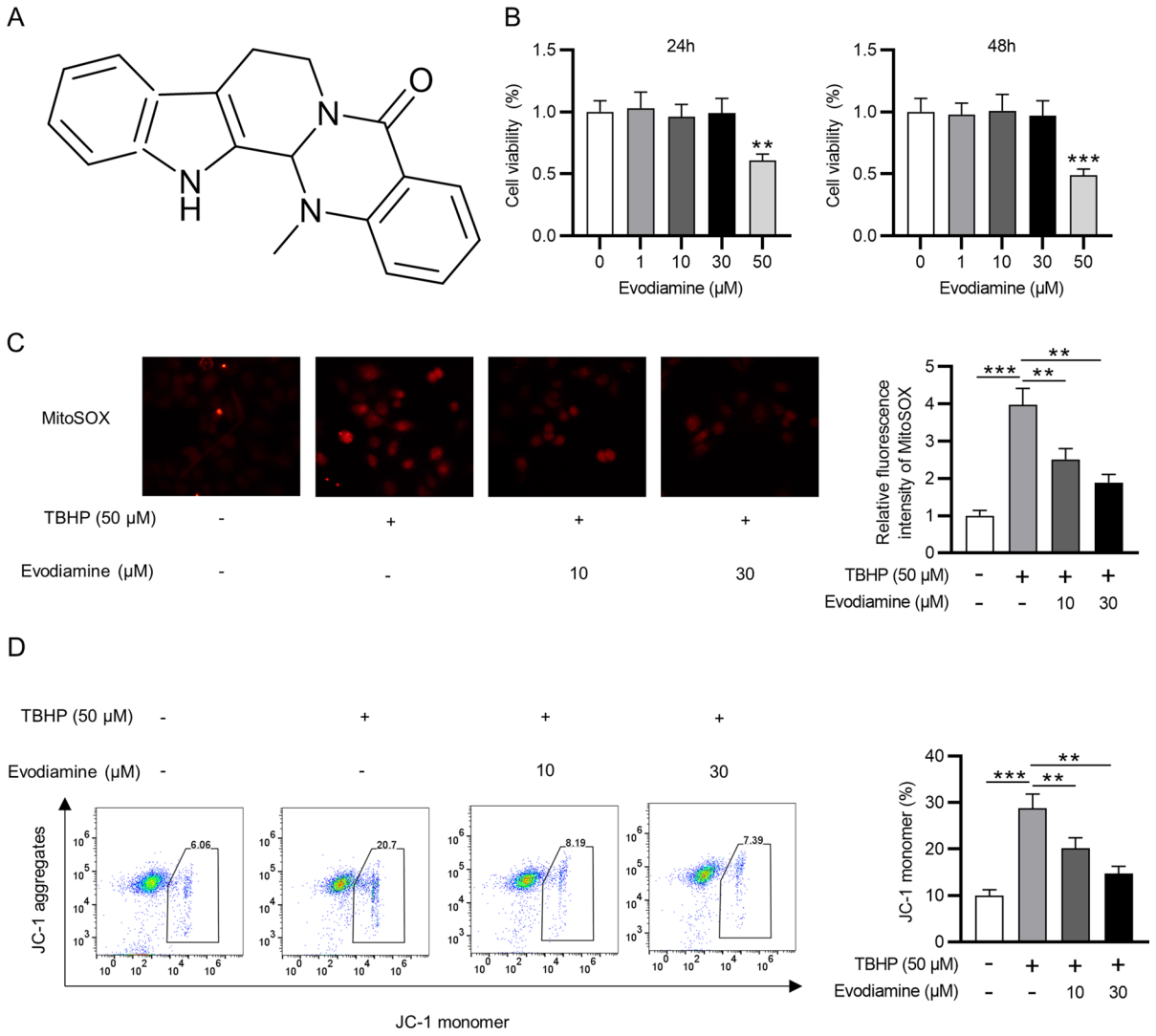

Fig. 1 Evodiamine alleviates TBHP-induced mitochondrial dysfunctions in NPCs. **A** Chemical structure of evodiamine. **B** The viability of cells exposed to 0 μM, 1 μM, 10 μM, 30 μM and 50 μM evodiamine at 24 h and 48 h was detected by CCK-8 assays. **C** The mitochondrial ROS in NPCs treated with evodiamine (10 μM and 30 μM) and then TBHP (50 μM) was measured through MitoSOX staining. **D** MMP in NPCs was measured by JC-1 staining and flow cytometry. Data are expressed as mean ± standard deviation of three independent experiments. $^{**}p < 0.01$, $^{***}p < 0.001$

Evodiamine reverses the promoting effects of TBHP on the ECM degradation

Then, we analyzed the effect of evodiamine on the anabolism of the ECM. The results of immunofluorescence staining demonstrated that the level of COL II was significantly decreased in TBHP-treated NPCs, whereas evodiamine reversed the inhibition (Fig. 2A). Additionally, as shown by western blotting, evodiamine treatment counteracted the inhibitory effect of TBHP on the level of aggrecan (Fig. 2B). The effect of evodiamine on ECM catabolism was also assessed by western blotting, and the results showed that the TBHP-induced increases in the levels of ECM catabolism markers (MMP-3, MMP-13 and ADAMTS-3) were reversed by evodiamine (Fig. 2B). Above findings show the protective effects of evodiamine against TBHP-induced ECM degradation.

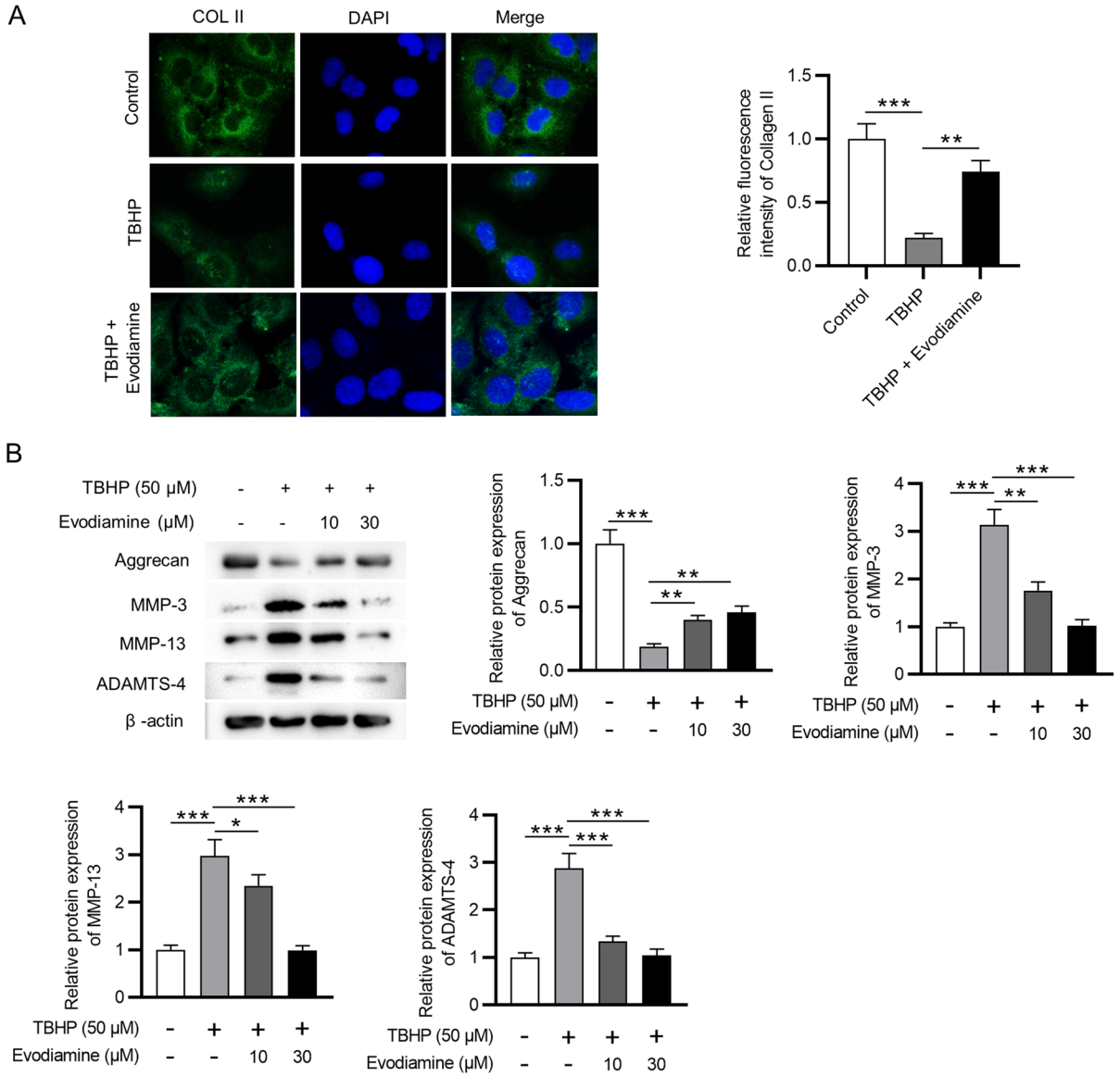

Fig. 2 Evodiamine ameliorates the TBHP-induced ECM degradation. **A** Immunofluorescence of collagen II expression after indicated treatment. **B** Western blotting was conducted to measure the protein levels of Aggrecan, MMP-3, MMP-13, and ADAMTS-4 in different groups. Data are expressed as mean± standard deviation of three independent experiments. $^{*}p < 0.05$, $^{**}p < 0.01$, $^{***}p < 0.001$

The TBHP-stimulated inflammatory responses are ameliorated by evodiamine

Next, we detected the effect of evodiamine on the production of proinflammatory cytokines. As shown by western blotting, the protein levels of iNOS and COX-2 were significantly increased by TBHP treatment, which were reduced by evodiamine (Fig. 3A). Additionally, the results of RT-qPCR revealed that the mRNA levels of TNF-α, IL-6 and IL-1β were upregulated under TBHP treatment, whereas evodiamine reversed the promotion (Fig. 3B). These data suggest that evodiamine suppresses the TBHP-induced inflammation in NPCs.

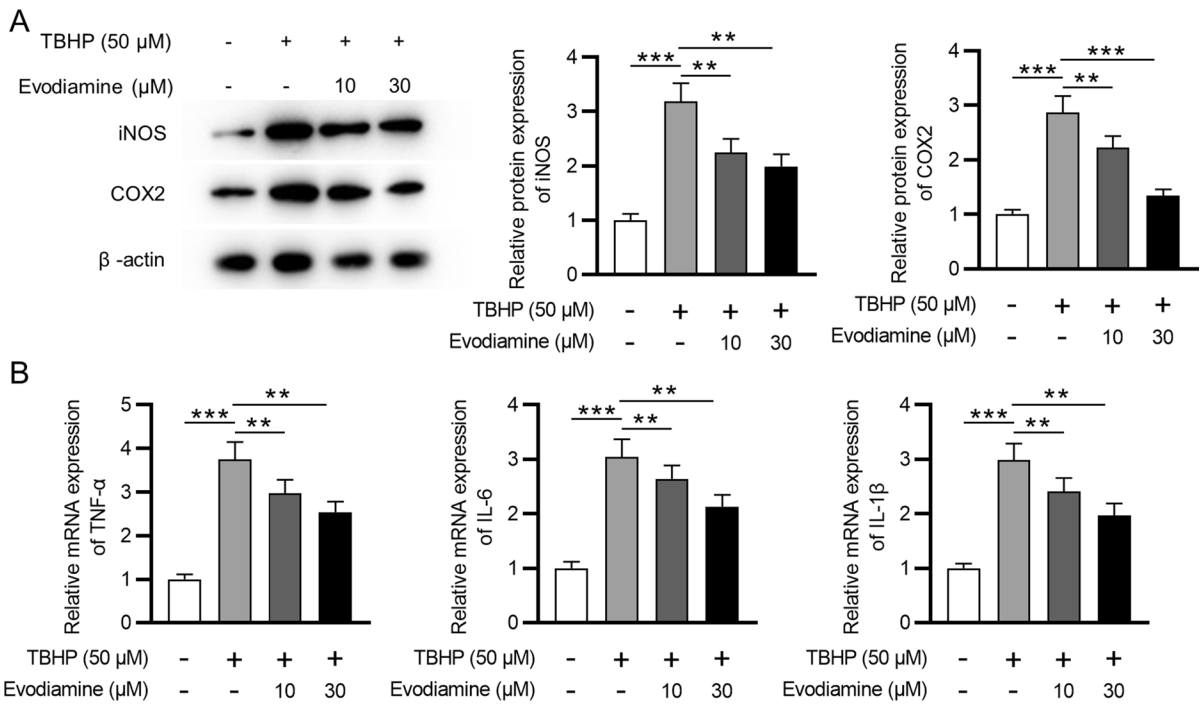

Fig. 3 The TBHP-stimulated inflammatory responses are ameliorated by evodiamine. **A** The protein levels of iNOS and COX2 were detected by western blotting. **B** The mRNA levels of TNF-α, IL-6 and IL-1β were measured by RT-qPCR. Data are expressed as mean ± standard deviation of three independent experiments. $^{**}p < 0.01$, $^{***}p < 0.001$

Evodiamine activates Nrf2 pathway and inhibits the TBHP-induced MAPK activation

To further confirm the underlying mechanism of evodiamine, we explored the effect of evodiamine on Nrf2/NQO1/HO-1 and MAPK by western blotting. The protein levels of Nrf2, NQO1 and HO-1 were not obviously changed after TBHP treatment, whereas evodiamine treatment led to significant increases in their protein levels dose-dependently (Fig. 4A, B). Additionally, the phosphorylation levels of p38, JNK and ERK were significantly enhanced in TBHP-stimulated NPCs, whereas evodiamine inhibited their phosphorylation (Fig. 4C). These results show that evodiamine activates the Nrf2/NQO1/HO-1 pathway and suppresses the TBHP-induced MAPK activation.

Evodiamine alleviates the IDD process in the puncture-induced rat model

To evaluate the effect of evodiamine on IDD in vivo, we induced IDD by puncturing the IVDs of rats. After surgery, the rats were intraperitoneally injected with 40 mg/kg or an equal volume of saline once a week for 4 weeks. The histological changes were detected by H&E staining, Safranin O/Fast Green staining and Alcian blue staining. H&E staining showed that the IVDs of the control group were full of NP tissues and that the surrounding annulus fibrosus remained intact, whereas needle puncture obviously changed the structure of the disc. The gel-like NP tissues were replaced by disorganized fibrocartilaginous tissues. The annulus fibrosus became invisible, and the distance between the vertebrae was narrowed. The vertebrae also exhibited bone destruction and hyperplasia. Notably, administration of evodiamine dramatically alleviated the observed disc degeneration. Safranin O/Fast Green and Alcian staining showed the proteoglycan and collagen contents. The color of the staining resulting from these two methods in the IDD group was much lighter than that in the control group, whereas the evodiamine group exhibited relatively intense staining compared with that in the IDD group, indicating that evodiamine partially reversed the observed disc degeneration. (Fig. 5A). We also used a histological score

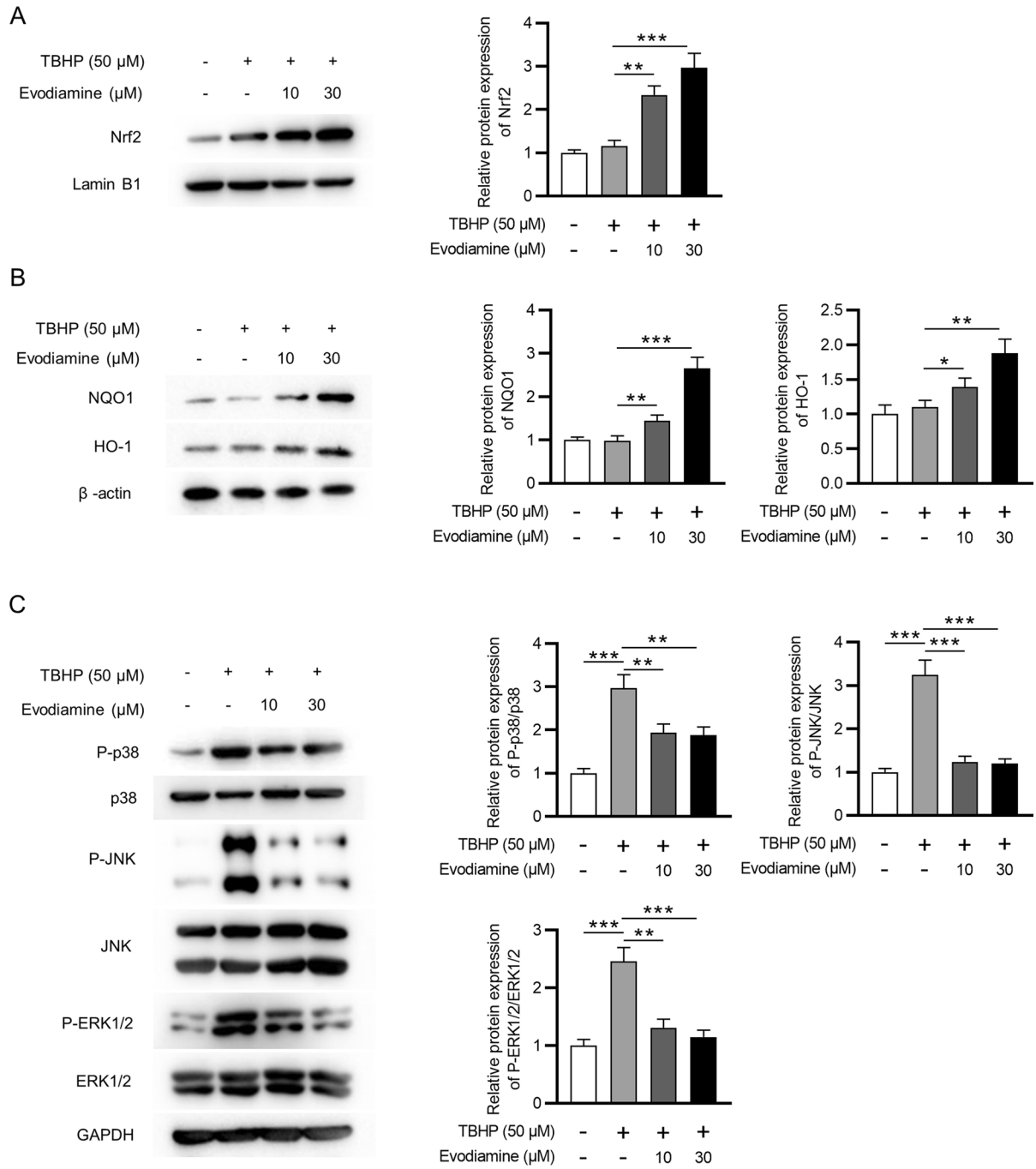

Fig. 4 Evodiamine mediates Nrf2 and MAPK pathways.**A**–**C** The protein levels of Nrf2, NQO1, HO-1, phosphorylated p38, phosphorylated JNK, phosphorylated ERK1/2 were measured by western blotting. Data are expressed as mean ± standard deviation of three independent experiments. *$p < 0.05$, **$p < 0.01$, ***$p < 0.001$

to compare the degree of degeneration in different groups. The results showed that the histological score was elevated by needle puncture, whereas evodiamine abolished the enhancing effects of needle puncture on histological score (Fig. 5B). Finally, we assessed the effect of evodiamine on the Nrf2/NQO1/HO-1 and

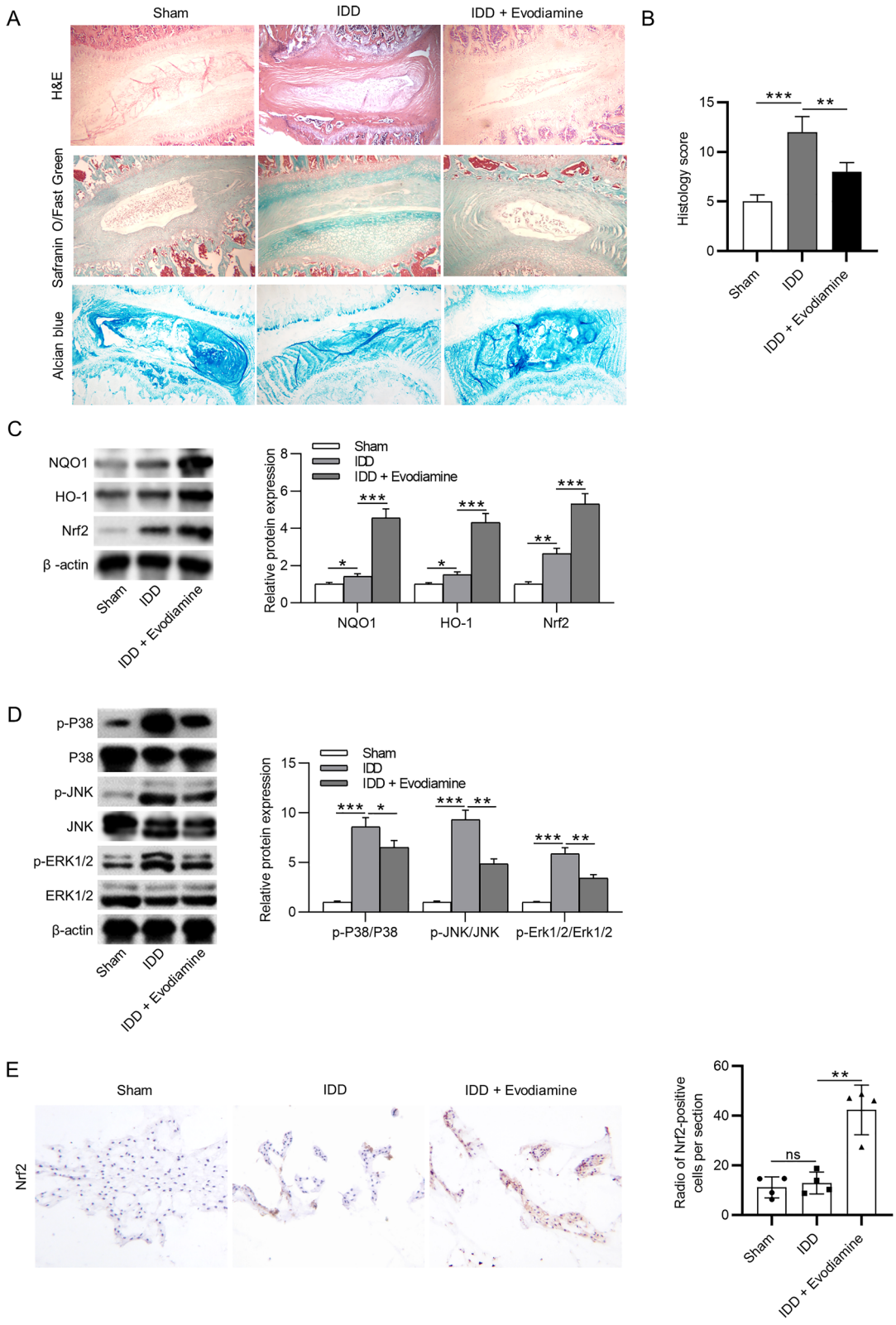
A
Sham
IDD
IDD + Evodiamine
H&E
Safranin O/Fast Green
Alcian blue
B
Histology score
C
NQO1
HO-1
Nrf2
β -actin
Relative protein expression
D
p-P38
P38
p-JNK
JNK
p-ERK1/2
ERK1/2
β-actin
p-P38/P38
p-JNK/JNK
p-Erk1/2/Erk1/2
E
Nrf2
Radio of Nrf2-positive cells per section
ns

◂**Fig. 5** Evodiamine alleviates IDD in vivo. **A** H&E, Safranin O/Fast Green and Alcian blue staining of IVDs. **B** Histological scores. **C** The protein levels of NQO1, HO-1 and Nrf2 were measured by western blotting. **D** The protein levels of phosphorylated p38, phosphorylated JNK and phosphorylated ERK1/2 were measured by western blotting. **E** The expression of Nrf2 was evaluated by immunohistochemistry staining. Data are expressed as mean ± standard deviation of 6 rats per group. $^{*}p < 0.05$, $^{**}p < 0.01$, $^{***}p < 0.001$

MAPK pathways in vivo. The results of western blotting revealed that evodiamine significantly increased the protein levels of NQO1, HO-1 and Nrf2 in the NP tissues of IDD models. Additionally, the needle puncture-induced promotion in the phosphorylation levels of p38, JNK and ERK were reversed by evodiamine (Fig. 5C, D). The results of immunohistochemistry analysis demonstrated that evodiamine administration induced the upregulation of Nrf2 in IDD models (Fig. 5E). These results show that evodiamine ameliorates the IDD progression in rats by activating the Nrf2/NQO1/HO-1 pathway and inactivating the MAPK pathway. The schematic diagram of the mechanisms underlying evodiamine involved in the progression of IDD was presented in Fig. 6. TBHP facilitated ROS generation, upregulated the levels of inflammatory mediators and promoted ECM degradation, whereas evodiamine inhibited ROS generation, inflammation and ECM degradation through the Nrf2 and MAPK pathways in TBHP-treated NPCs.

Discussion

IDD is a major cause of low back pain. Initial treatment for IDD is still limited to conservative methods, and effective therapeutic drugs are lacking. It is a priority to facilitate the drug development and clinical treatment strategies. Evodiamine is a quinozole alkaloid that is mainly isolated from the fruits of *Evodia rutaecarpa*. Its anti-inflammatory and antioxidant activities have been well established (Wu and Chen 2019; Fan et al. 2017; Eraslan et al. 2019). Evodiamine can also attenuate adjuvant-induced arthritis in rats by inhibiting synovial inflammation and restoring the Th17/Treg balance (Zhang et al. 2020), alleviate the dexamethasone-induced osteoporosis in Zebrafish (Yin et al. 2019), and inhibit osteoclastogenesis and prevent ovariectomy-induced bone loss in mice (Jin et al. 2019). However, the biological functions of evodiamine in IDD progression remain uncertain. In the current study, we detected the effect of evodiamine in TBHP-treated NPCs and puncture-induced IDD models in rats.

ROS has been reported to exacerbate diverse pathological processes underlying IDD, including stimulating inflammation and facilitating the apoptosis and senescence of NPCs. ROS generation mainly occurs in mitochondria. Mitochondrial dysfunction is a primary contributor of excessive ROS production (Gruber et al. 2013). TBHP is a kind of organic peroxide that is more stable than ordinary hydrogen peroxide. Therefore, we treated NPCs with TBHP to stimulate a high-ROS extracellular environment (Liu et al. 2020). Evodiamine is found to suppress ROS production in LPS-treated NRK-52E cells (Shi et al. 2019) and high free fatty acids-exposed human umbilical vein endothelial cells (Xue et al. 2018). Additionally, evodiamine maintains the mitochondrial antioxidant functions in rats with paclitaxel-induced neuropathic pain (Wu and Chen 2019). In the current study, we found that evodiamine reduced the mitochondria-derived ROS and MMP in TBHP-treated NPCs.

ECM degradation and inflammation are crucial characteristics of the degenerative process (Clouet et al. 2009). Excessive catabolism and inadequate anabolism induce ECM degradation. This imbalance is manifested by ADAMTS-4, MMP-3, MMP-13, collagen II and aggrecan. A previous study shows that the increased expression of iNOS, COX-2 and MMP-13 and the degradation of aggrecan and collagen II are alleviated by evodiamine in IL-1β-activated mouse chondrocytes (Xian et al. 2022). Additionally, evodiamine mitigates LPS-induced ECM degradation and inflammation in NPCs (Kuai and Zhang 2022). In the current study, we found that evodiamine rescued the TBHP-induced decreased collagen II and aggrecan expression levels. Additionally, the elevated levels of MMP-3, MMP-13 and ADAMTS-4 induced by TBHP were decreased by evodiamine administration, suggesting that evodiamine alleviated the TBHP-induced ECM degradation. Moreover, the levels of COX-2, iNOS, TNF-α, IL-6 and IL-1β were increased after TBHP treatment, while evodiamine administration decreased their expression levels. These results demonstrated that evodiamine alleviated the TBHP-induced ECM degradation and inflammatory responses in NPCs.

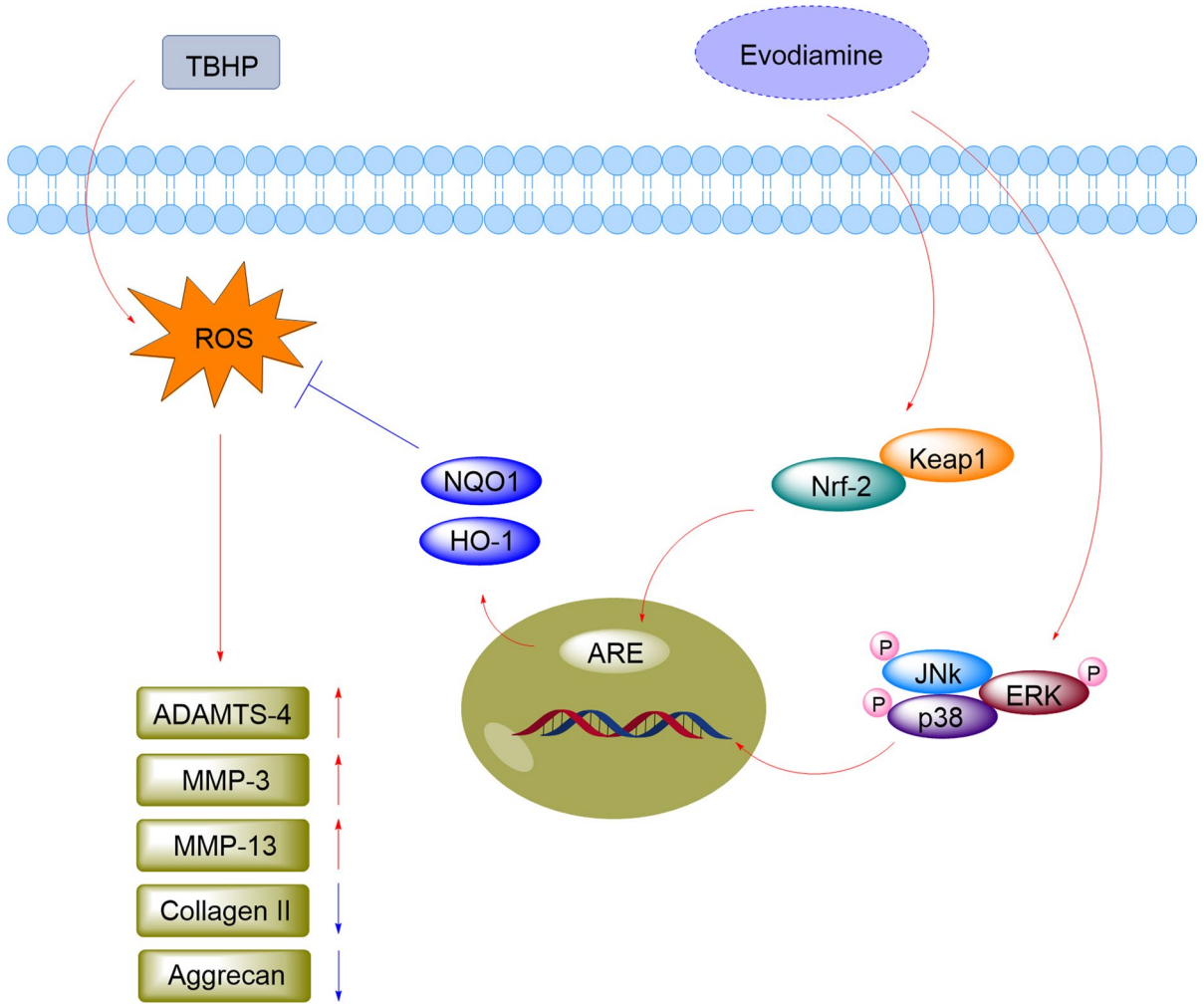

Fig. 6 The schematic diagram of the mechanisms underlying evodiamine involved in the progression of IDD

Nrf2 mediates antioxidant response by regulating the expression of ARE-containing genes that maintain redox homeostasis and counteract the oxidative stress. NQO1 and HO-1 are two downstream antioxidant enzymes of Nrf2. A previous study has suggested that evodiamine enhances the nuclear translocation of Nrf2 and upregulates HO-1 level in BV2 cells (Meng et al. 2021). In the current study, we discovered that evodiamine increased the levels of Nrf2, NQO1 and HO-1 in the TBHP-treated NPCs, activating the Nrf2/NQO1/HO-1 pathway.

The activated MAPKs (p38 kinase, ERK and JNK) lead to the accumulation of MMPs and ADAMTSs during IDD. As reported, evodiamine inhibits the MAPK pathway in the lipopolysaccharide-induced mouse mammary epithelial cells (Yang et al. 2022), the infection-induced gastric adenocarcinoma cells (Yang et al. 2021) and the hepatocellular cancer cells (Guo et al. 2018). In the current study, we found that evodiamine decreased the ratios of p-p38/p38, p-JNK/JNK, and p-ERK1/2/ERK1/2, inactivating the MAPK pathway.

In summary, this study demonstrated that evodiamine alleviated IDD progression by inhibiting mitochondrial ROS generation, ECM degradation and inflammatory responses through activating the Nrf2/NQO1/HO-1 pathway and inactivating the MAPK pathway. There are limitations to this study. First, experiments were only performed at only one time point; thus, additional time points should be

investigated. Second, the inhibitors of Nrf2 and MAPK could be used in the puncture-induced rat model to verify the effect of evodiamine in IDD. Third, although evodiamine exhibited anti-inflammatory, antioxidant and ECM protective effects in the present study, the potential for treatment and possible complications of evodiamine on human diseases require additional examination through clinical research. Fourth, due to limited funding, we did not provide MRI or X-ray results in this study. Although this study exists limitations, we believed that evodiamine could be a promising option for IDD treatment.

Acknowledgements We appreciate the support from the Wuhan Hospital of Traditional Chinese Medicine.

Author contributions XG and TX were the main designers of this study. XG, TX, RP, WH, SD performed the experiments and analyzed the data. XG and TX drafted the manuscript. All authors read and approved the final manuscript.

Funding This work was supported by Wuhan Municipal Health Commission (approval number: WZ15B09).

Declarations

Conflict of interest The authors have not disclosed any conflict of interests.

Ethical approval The experimental protocols were granted approval from the Ethics Committee of Wuhan Myhalic Biotechnology Co., Ltd (No. 202007109) and abided by the National Institutes of Health Guide for the Care and Use of Laboratory Animals.

References

Bai Z et al (2020) Protective effects of autophagy and NFE2L2 on reactive oxygen species-induced pyroptosis of human nucleus pulposus cells. Aging 12:7534–7548

Bermudez-Lekerika P et al (2022) Immuno-modulatory effects of intervertebral disc cells. Front Cell Dev Biol 10:924692

Clouet J et al (2009) The intervertebral disc: from pathophysiology to tissue engineering. Joint Bone Spine 76:614–618

Dimozi A et al (2015) Oxidative stress inhibits the proliferation, induces premature senescence and promotes a catabolic phenotype in human nucleus pulposus intervertebral disc cells. Eur Cell Mater 30:89–102

Dydyk AM, Ngnitewe Massa R, Mesfin FB (2023) Disc herniation. In: StatPearls. 2023, StatPearls Publishing LLC, Treasure Island

Eraslan E et al (2019) Evodiamine alleviates kidney ischemia reperfusion injury in rats: a biochemical and histopathological study. J Cell Biochem 120:17159–17166

Fan X et al (2017) Evodiamine inhibits zymosan-induced inflammation in vitro and in vivo: inactivation of NF-κB by inhibiting IκBα phosphorylation. Inflammation 40:1012–1027

Ge J et al (2020) The protein tyrosine kinase inhibitor, genistein, delays intervertebral disc degeneration in rats by inhibiting the p38 pathway-mediated inflammatory response. Aging 12:2246–2260

Global, regional, and national incidence, prevalence, and years lived with disability for 310 diseases and injuries, 1990–2015: a systematic analysis for the global burden of disease study 2015. Lancet, 2016. 388:1545–1602

Global, regional, and national incidence, prevalence, and years lived with disability for 328 diseases and injuries for 195 countries, 1990–2016: a systematic analysis for the Global Burden of Disease Study 2016 Lancet, 390:1211–1259 (2017)

Gruber HE et al (2013) Mitochondrial bioenergetics, mass, and morphology are altered in cells of the degenerating human annulus. J Orthop Res 31:1270–1275

Guo XX et al (2018) Evodiamine induces apoptosis in SMMC-7721 and HepG2 cells by suppressing NOD1 signal pathway. Int J Mol Sci. https://doi.org/10.3390/ijms19113419

Guo Q et al (2021) Targeting STING attenuates ROS induced intervertebral disc degeneration. Osteoarthritis Cartilage 29:1213–1224

Hayes AJ, Benjamin M, Ralphs JR (2001) Extracellular matrix in development of the intervertebral disc. Matrix Biol 20:107–121

Jin H et al (2019) Evodiamine inhibits RANKL-induced osteoclastogenesis and prevents ovariectomy-induced bone loss in mice. J Cell Mol Med 23:522–534

Johnson GL, Lapadat R (2002) Mitogen-activated protein kinase pathways mediated by ERK, JNK, and p38 protein kinases. Science 298:1911–1912

Jordan J, Konstantinou K, O'Dowd J (2011) Herniated lumbar disc. BMJ Clin Evid 2011:1118

Kepler CK et al (2013) Expression and relationship of proinflammatory chemokine RANTES/CCL5 and cytokine IL-1β in painful human intervertebral discs. Spine (Phila Pa 1976) 38:873–880

Kong M et al (2021) Myocardin–related transcription factor a nuclear translocation contributes to mechanical overload–induced nucleus pulposus fibrosis in rats with intervertebral disc degeneration. Int J Mol Med 48:1–13

Kuai J, Zhang N (2022) Upregulation of SIRT1 by evodiamine activates PI3K/AKT pathway and blocks intervertebral disc degeneration. Mol Med Rep 26:1–8

Le Maitre CL, Freemont AJ, Hoyland JA (2005) The role of interleukin-1 in the pathogenesis of human intervertebral disc degeneration. Arthritis Res Ther 7:R732–R745

Lee C (2018) Therapeutic modulation of virus-induced oxidative stress via the Nrf2-dependent antioxidative pathway. Oxid Med Cell Longev. https://doi.org/10.1155/2018/6208067

Li Y et al (2022) Silencing ATF3 might delay TBHP-induced intervertebral disc degeneration by repressing NPC ferroptosis, apoptosis, and ECM degradation. Oxid Med Cell Longev 2022:4235126

Liu X et al (2020) Sodium butyrate protects against oxidative stress in human nucleus pulposus cells via elevating

PPARγ-regulated klotho expression. Int Immunopharmacol 85:106657
Livak KJ, Schmittgen TD (2001) Analysis of relative gene expression data using real-time quantitative PCR and the 2(-delta delta C(T)) method. Methods 25:402–408
Mao HJ et al (2011) The effect of injection volume on disc degeneration in a rat tail model. Spine (Phila Pa 1976) 36:E1062–E1069
Meng T et al (2021) Evodiamine inhibits lipopolysaccharide (LPS)-induced inflammation in BV-2 cells via regulating AKT/Nrf2-HO-1/NF-κB signaling axis. Cell Mol Neurobiol 41:115–127
Millward-Sadler SJ et al (2009) Regulation of catabolic gene expression in normal and degenerate human intervertebral disc cells: implications for the pathogenesis of intervertebral disc degeneration. Arthritis Res Ther 11:R65
Raj PP (2008) Intervertebral disc: anatomy-physiology-pathophysiology-treatment. Pain Pract 8:18–44
Risbud MV, Shapiro IM (2014) Role of cytokines in intervertebral disc degeneration: pain and disc content. Nat Rev Rheumatol 10:44–56
Shi Y et al (2019) Protective effects of evodiamine against LPS-induced acute kidney injury through regulation of ROS-NF-κB-mediated inflammation. Evid Based Complement Alternat Med 2019:2190847
Shin N et al (2020) p66shc siRNA-Encapsulated PLGA nanoparticles ameliorate neuropathic pain following spinal nerve ligation. Polymers (Basel). https://doi.org/10.3390/polym12051014
Son JK, Chang HW, Jahng Y (2015) Progress in studies on rutaecarpine. II.—synthesis and structure-biological activity relationships. Molecules 20:10800–10821
Wang Q et al (2021) Evodiamine protects against airway remodelling and inflammation in asthmatic rats by modulating the HMGB1/NF-κB/TLR-4 signalling pathway. Pharm Biol 59:192–199
Wu P, Chen Y (2019) Evodiamine ameliorates paclitaxel-induced neuropathic pain by inhibiting inflammation and maintaining mitochondrial anti-oxidant functions. Hum Cell 32:251–259
Xian S et al (2022) The protective effect of evodiamine in osteoarthritis: an in vitro and in vivo study in mice model. Front Pharmacol 13:899108
Xin J et al (2022) Treatment of intervertebral disc degeneration. Orthop Surg 14:1271–1280
Xue Y et al (2018) Evodiamine attenuates P2X(7)-mediated inflammatory injury of human umbilical vein endothelial cells exposed to high free fatty acids. Oxid Med Cell Longev 2018:5082817
Yang JY et al (2021) Evodiamine inhibits *Helicobacter pylori* Growth and *Helicobacter pylori*-induced inflammation. Int J Mol Sci. https://doi.org/10.3390/ijms22073385
Yang Y et al (2022) Evodiamine relieve LPS-induced mastitis by inhibiting AKT/NF-κB p65 and MAPK signaling pathways. Inflammation 45:129–142
Ye C et al (2021) Evodiamine alleviates lipopolysaccharide-induced pulmonary inflammation and fibrosis by activating apelin pathway. Phytother Res 35:3406–3417
Yin H et al (2019) Preventive effects of evodiamine on dexamethasone-induced osteoporosis in zebrafish. Biomed Res Int 2019:5859641
Youle RJ, van der Bliek AM (2012) Mitochondrial fission, fusion, and stress. Science 337:1062–1065
Zhang H et al (2020) Evodiamine attenuates adjuvant-induced arthritis in rats by inhibiting synovial inflammation and restoring the Th17/treg balance. J Pharm Pharmacol 72:798–806